Supporting Information for:

Probing ^{27}Al-^{13}C Proximities in Metal-Organic Frameworks using Dynamic Nuclear Polarization enhanced NMR Spectroscopy

Frédérique Pourpoint*, Aany Sofia Lilly Thankamony, Christophe Volkringer, Thierry Loiseau, Julien Trébosc, Fabien Aussenac, Diego Carnevale, Geoffrey Bodenhausen, Hervé Vezin, Olivier Lafon* and Jean-Paul Amoureux

Corresponding authors:

frederique.pourpoint@ensc-lille.fr

olivier.lafon@univ-lille1.fr

EPR experiments

MIL-100(Al) was synthesized following the literature procedure.[1] It was first heated at 150°C overnight to eliminate adsorbed water trapped within the pores of the material. EPR sample was prepared by adding about 15 µL of 16 mM TOTAPOL dissolved in water with natural isotopic abundance to about 20 mg of MIL-100(Al) dry powder. Just after the addition of TOTAPOL solution, 9 GHz continuous-wave EPR spectra were recorded every minute during 550 min using a Bruker Biospin ELEXYS E580E spectrometer. The spectra were recorded with 2 mW microwave power and 0.5 G of amplitude modulation.

Sample preparation for DNP measurement

The sample for solid-state DNP NMR experiments was prepared at room temperature by impregnating dry MIL-100(Al) with a 16 mM TOTAPOL dissolved in water with natural isotopic abundance. Even though other impregnation solvents and polarizing agents were tested, including (i) 90/10 (w/w) mixture of ^2H_2O and H_2O (ii) 78/14/8 (w/w/w) mixture of [$^2H_6$]-DMSO, ^2H_2O and H_2O, the impregnation of MIL-100(Al) with these radical solutions resulted in lower DNP enhancement. Typically an aliquot of 60 µL of radical solution was added to cover about 30 mg of MIL-100 (Al) dry powder. The mixture was stirred vigorously and kept at room temperature for one day. After this saturation, the mixture was centrifuged for 5 min at 12110×*g* and the supernatant was pipetted. The remaining wet powder was packed into a thick-walled 3.2 mm zirconia rotor. Zirconia rotors were employed to avoid ^{27}Al background signal of sapphire rotor.

DNP and standard NMR measurements at 100 K

The solid-state NMR experiments at 100 K enhanced or not by DNP were obtained at 9.4 T (400 MHz for protons) using a Bruker BioSpin Avance III DNP NMR spectrometer, equipped with a gyrotron generating a continous 263 GHz µw irradiation. The µw irradiation was transmitted through a corrugated waveguide to a triple resonance ^{1}H/X/Y MAS probe for 3.2 mm rotors. The μw power at the position of the sample was approximately 6 W. NMR spectra with μw irradiation "on" and "off" were acquired at ν_r = 10 kHz and sample temperature of ca. 100 K, which was stabilized by a Bruker BioSpin MAS cooling system.

The employed NMR pulse sequences are depicted in **Fig.S2**. The ^{1}H rf-amplitude for 90°-pulse was 89 kHz. For ^{1}H→^{13}C CP-MAS transfer, the cross-polarization time was 3.2 ms, the ^{1}H rf field amplitude was linearly ramped from 42 to 85 kHz, whereas the ^{13}C rf field amplitude was constant and equal to 42 kHz. For ^{1}H→^{27}Al CP-MAS transfer, the cross-polarization time was 800 μs, the ^{1}H rf amplitude was 33 kHz, whereas the ^{27}Al rf amplitude was equal to 7.6 kHz (central transition selective pulse). SPINAL-64[3] ^{1}H decoupling was applied during the acquisition of ^{13}C spectra with an rf amplitude of 89 kHz. No ^{1}H decoupling was applied during the acquisition of ^{27}Al spectra. The ^{1}H→^{13}C and ^{1}H→^{27}Al CP-MAS spectra typically resulted from the accumulation of 64 transients with a recovery delay of 1 s, leading to a total experimental time of 1 min. Other parameters of direct ^{1}H, ^{13}C MAS experiments and ^{27}Al Hahn-echo experiments are given in Figs.S3 and S4. The ^{1}H and ^{13}C chemical shifts were referenced to tetramethylsilane (TMS) at 0 ppm, whereas the ^{27}Al chemical shifts were referenced to 1 M $AlCl_3$ aqueous solution.

DNP-enhanced ^{13}C-{^{27}Al} and ^{27}Al-{^{13}C} CP-*D*-HMQC 2D spectra and ^{27}Al-^{13}C S-RESPDOR curves were recorded with μw irradiation. SFAM-1 recoupling was chosen to reintroduce the ^{13}C-^{27}Al dipolar couplings owing to its high robustness, its large scaling factor of the recoupled dipolar interaction and the negligible ^{13}C-^{13}C dipolar couplings in natural abundance.[4] The rf field amplitude of ^{13}C 90° and 180° pulses as well as the rf peak amplitude of SFAM-1 recoupling were equal to 42 kHz. The rf field amplitude of ^{27}Al 90° and 180° CT-selective pulses was 5 kHz for CP-*D*-HMQC experiment, whereas the amplitude of ^{27}Al saturation pulse in S-RESPDOR was 46 kHz. The sum of the two SFAM-1 recoupling periods, τ, was equal to 6 ms in CP-*D*-HMQC experiment and was varied from 0 to 5 ms in *S*-RESPDOR experiments. Continuous wave ^{1}H decoupling with an rf field amplitude of 89 kHz was applied during SFAM-1 recoupling periods. SPINAL-64 ^{1}H decoupling with an rf field amplitude of 89 kHz was also applied during the indirect evolution period, t_1, of CP-*D*-HMQC experiments. The recovery delays of these experiments was 1 s. The number of transients, the number of t_1 or τ increments and the total experimental times were equal to (640, 20, 7.1 h) for ^{13}C-{^{27}Al} CP-*D*-HMQC, (640, 26, 16 h) for S-RESPDOR and (4096, 20, 39 h) for ^{27}Al-{^{13}C} CP-*D*-HMQC.

^{27}Al-^{13}C S-RESPDOR experiment at 100 K without microwave irradiation was also acquired for dry MIL-100(Al). The experimental parameters are identical to those employed for DNP-enhanced S-RESPDOR, except for the number of scans, which is 3616.

Standard solid-state NMR measurements at room temperature

^{27}Al-{^{13}C} CP-*D*-HMQC 2D spectra and ^{27}Al-^{13}C S-RESPDOR curves were also aquired at room temperature without microwave irradiation. The experimental parameters are identical to those of DNP-enhanced experiments, except the number of scans, which was equal at room temperature to 2048 and 3616, corresponding to 17 and 61 h, for CP-*D*-HMQC and S-RESPDOR, respectively.

Spin dynamics simulations

The simulated ^{27}Al-^{13}C S-RESPDOR curves in Fig.**S9** were calculated as follows. For each ^{13}C*i* signal, the simulated ^{27}Al-^{13}C S-RESPDOR curve is the sum of the eleven simulated S-RESPDOR signal fractions for the eleven crystallographically inequivalent C*i* sites contained in the unit cell. The S-RESPDOR signal fraction was simulated for each crystallographically inequivalent site using SIMPSON software[5] and a spin system consisting of one ^{13}C nucleus surrounded by its two nearest ^{27}Al neighbours in the MIL-100(Al) crystal structure. The ^{27}Al quadrupolar interaction was considered up to the second-order and the quadrupolar coupling constant, C_Q, and the asymmetry parameters of the electric field gradient, η_Q, were equal to 4.6 MHz and 0.5, respectively. The parameters of the S-RESPDOR pulse sequence were identical to the experimental ones. The powder average was calculated using 168 $\{\alpha_{MR},\beta_{MR}\}$pairs and 13 γ_{MR} angles. The 168 $\{\alpha_{MR},\beta_{MR}\}$pairs, which relate the molecular and rotor frames, were selected according to the REPULSION scheme.

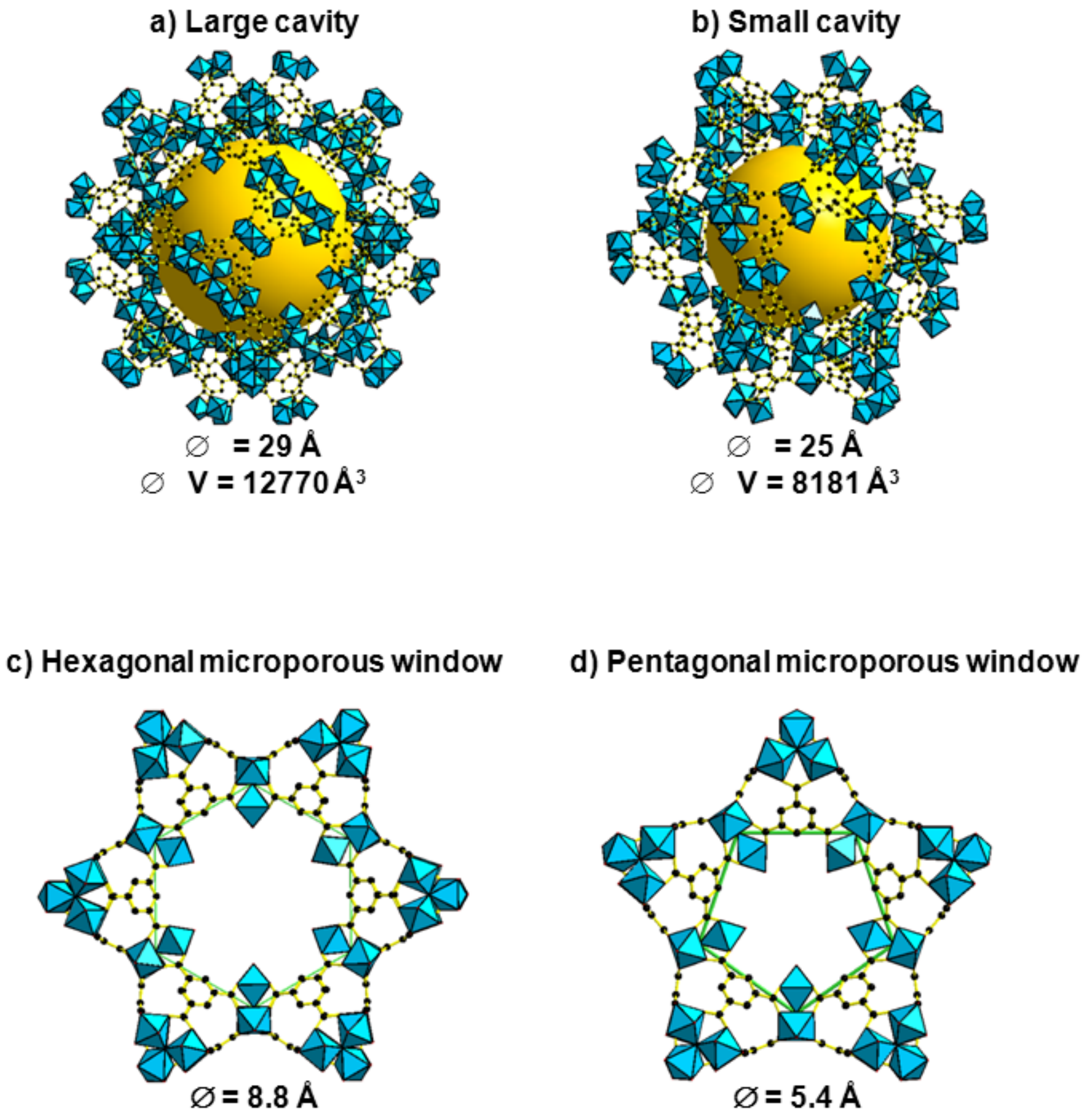

Fig. S1: Representations of the (a) large and (b) small cavities of MIL-100(Al). Large cavities display both (c) hexagonal and (d) pentagonal apertures, respectively, whereas small cavities only display pentagonal apertures. The inner diameter and the volume of the cavities are indicated below the subfigures a and b, whereas the diameter of the apertures is given below subfigures c and d.

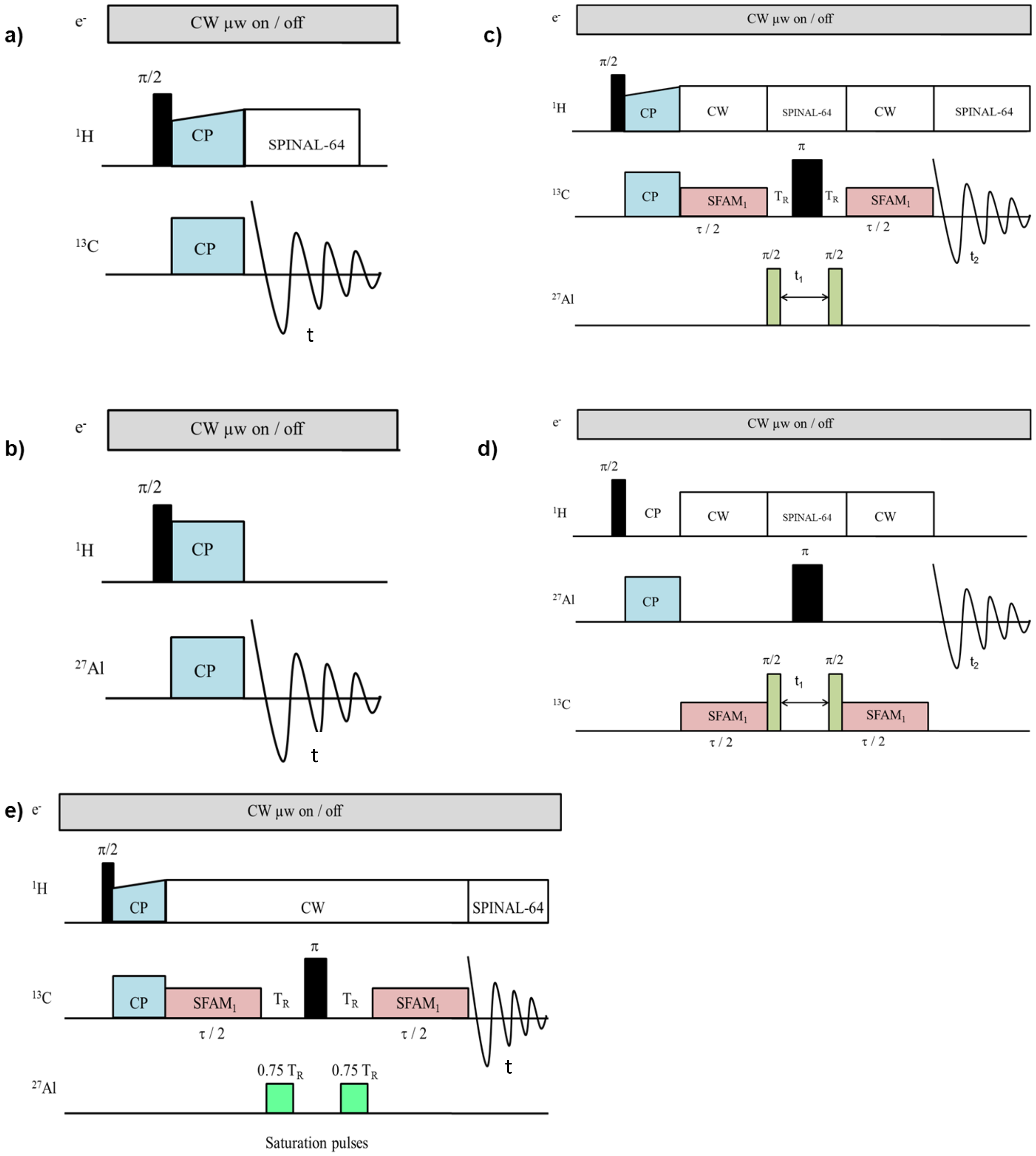

Fig.S2 NMR pulse sequences for: (a) 1D $^{1}H \rightarrow ^{13}C$ CP-MAS, (b) 1D $^{1}H \rightarrow ^{27}Al$ CP-MAS, (c) 2D ^{13}C-{^{27}Al} CP-*D*-HMQC, (d) 2D ^{27}Al-{^{13}C} CP-*D*-HMQC, and (e) ^{27}Al-^{13}C CP-S-RESPDOR. The phase cycling of CP-D-HMQC and CP-S-RESPDOR are given in refs [4] and [6], respectively.

DNP enhancement for CP-MAS if TOTAPOL does not enter into MIL-100(Al) cavities

To confirm the diffusion of TOTAPOL into the large cavities of MIL-100(Al), we use *reductio ad absurbum*: we assume that TOTAPOL molecules do not penetrate into the MIL-100(Al) crystals and are relagated into the interparticle voids. The ^{1}H polarization of the frozen water within the interparticle voids is assumed to be uniform and equal to $P_{\mathrm{eq}}\,\varepsilon_{on/off}^{scan}(R)$ where P_{eq} is the ^{1}H polarization at thermal equilibrium and $\varepsilon_{on/off}^{scan}(R)$ is the steady-state enhancement per scan produced by microwave irradiation for the protons within the interparticle voids. This DNP-enhanced ^{1}H polarization can only enter into the bulk of MIL-100(Al) crystals via ^{1}H-^{1}H spin diffusion. We assume an uniform proton density within the MIL-100(Al) crystals. This proton density can be estimated from the empirical formula and the unit cell volume of hydrated MIL-100(Al) to be equal to $n(^1\mathrm{H}) = 4.3\times10^2$ Å^3.

The average ^{1}H-^{1}H distance is thus equal to

$$d_{HH} = n\left(^1\mathrm{H}\right)^{-1/3} \approx 0.3\ \mathrm{nm} \tag{S1}$$

The average dipolar coupling constant, b_{HH}, in rad.s^{-1} between two protons at a distance d_{HH} is

$$b_{HH} = -\frac{\mu_0}{4\pi}\frac{\gamma_H^2\hbar}{d_{HH}^3} \tag{S2}$$

where μ_0 is the vaccum permeability and all physical quantities are expressed in SI units. Under MAS condition, the effective dipolar coupling, ν_{d}, expressed in Hz can be estimated as[7]

$$\nu_d = \frac{b_{HH}^2}{4\pi^2\nu_r} \tag{S3}$$

The ^{1}H-^{1}H spin diffusion coefficient, D, is given by

$$D = d_{HH}^2\pi\nu_d \tag{S4}$$

Using Eqs.S1 to S4, we obtain $D = 6.8\times10^2$ nm^2.s^{-1}. This spin diffusion coefficient can be used to estimate the distribution of ^{1}H polarization within MIL-100(Al) crystals. These crystals have an octahedral shape and an average length of 1 μm.[8] However, for the sake of simplicity, the crystals are assumed to be spheres with a radius $R = 500$ nm and the diffusion to be radial. We also assume that all ^{1}H nuclei within the bulk MIL-100(Al) crystal have an identical longitudinal relaxation time of $T_1 = 0.7$ s. The ^{1}H polarization evolves under longitudinal ^{1}H relaxation and ^{1}H-^{1}H spin diffusion. Under the above assumption, the evolution of ^{1}H polarization within the bulk MIL-100(Al) crystal is given by[9]

$$\frac{\partial P(r,t)}{\partial t} = \frac{D}{r}\frac{\partial^2\left[rP(r,t)\right]}{\partial r^2} - \frac{P(r,t)-P_{eq}}{T_1}. \tag{S5}$$

Introducing $f(r,t) = r[P(r,t) - P_{eq}]$, Eq.S5 can be written as

$$\frac{\partial f(r,t)}{\partial t} = D\frac{\partial^2[f(r,t)]}{\partial r^2} - \frac{f(r,t)}{T_1} \tag{S6}$$

In the steady-state, all the physical quantities, including *f*, are time-independent and Eq.S6 becomes

$$\frac{\partial^2[f(r)]}{\partial r^2} - \frac{f(r)}{l_D^2} = 0 \tag{S7}$$

where $l_D = \sqrt{DT_1}$ is the diffusion length. Here, l_D is about 22 nm. Furthermore, the ^{1}H polarization at the center of the crystal, *P*(0), is finite, whereas it is equal to $P_{eq}\,\varepsilon_{on/off}^{scan}(R)$ at the surface of the crystal. Therefore, boundary conditions for *f* function are

$$f(0) = 0 \quad \text{and} \quad f(R) = R\left[\varepsilon_{on/off}^{scan}(R) - 1\right]P_{eq}\ . \tag{S8}$$

Solving Eq.S7 with the above boundary conditions leads to

$$P(r) = P_{eq}\left\{1 + \left[\varepsilon_{on/off}^{scan}(R) - 1\right]\frac{R}{r}\sinh\left(\frac{r}{l_D}\right)/\sinh\left(\frac{R}{l_D}\right)\right\} \tag{S9}$$

The enhancement per scan produced by μw irradiation is equal to the ratio of the polarization over the volume of the crystal with and without μw irradiation:

$$\varepsilon_{on/off}^{scan} = \frac{3}{4\pi R^3 P_{eq}}\int_0^R P(r)dR = 1 + 3\left[\varepsilon_{on/off}^{scan}(R) - 1\right]\frac{l_D}{R}\left\{\coth\left(\frac{R}{l_D}\right) - \frac{l_D}{R}\right\} \tag{S10}$$

For mesoporous systems, in which TOTAPOL molecules enter into the mesopores, we have measured enhancements per scan due to μw irradiation ranging from 11 to 30 for CP-MAS experiments.[7,9-11] Therefore, $\varepsilon_{on/off}^{scan}(R)$ value must fall within the above interval, which leads to $\varepsilon_{on/off}^{scan}$ values for MIL-100(Al) crystal ranging from 2.2 to 4.6. These estimates are not consistent with the experimental value $\varepsilon_{on/off}^{scan} = 8.5$ (see Fig.1 and S3). Hence, the TOTAPOL molecule must penetrate into the MIL-100(Al) cavities.

DNP-enhanced direct excitation experiments

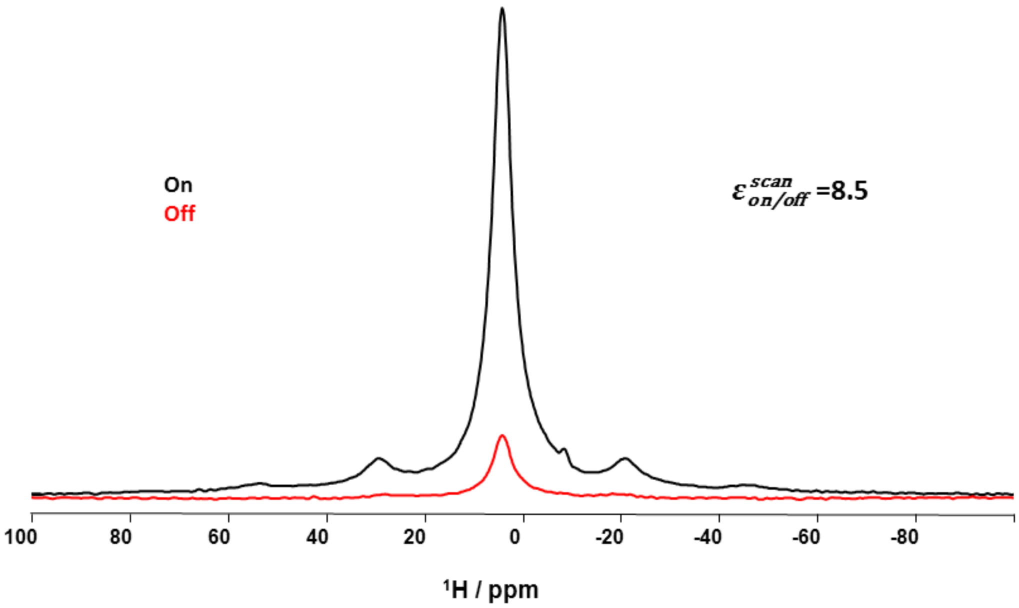

Fig.S3 ^{1}H MAS spectra of MIL-100(Al) recorded with (black) and without (red) μw irradiation. The spectra resulted from the accumulation of 64 transients with a recovery delay of 1 s, leading to a total experimental time of 1 min.

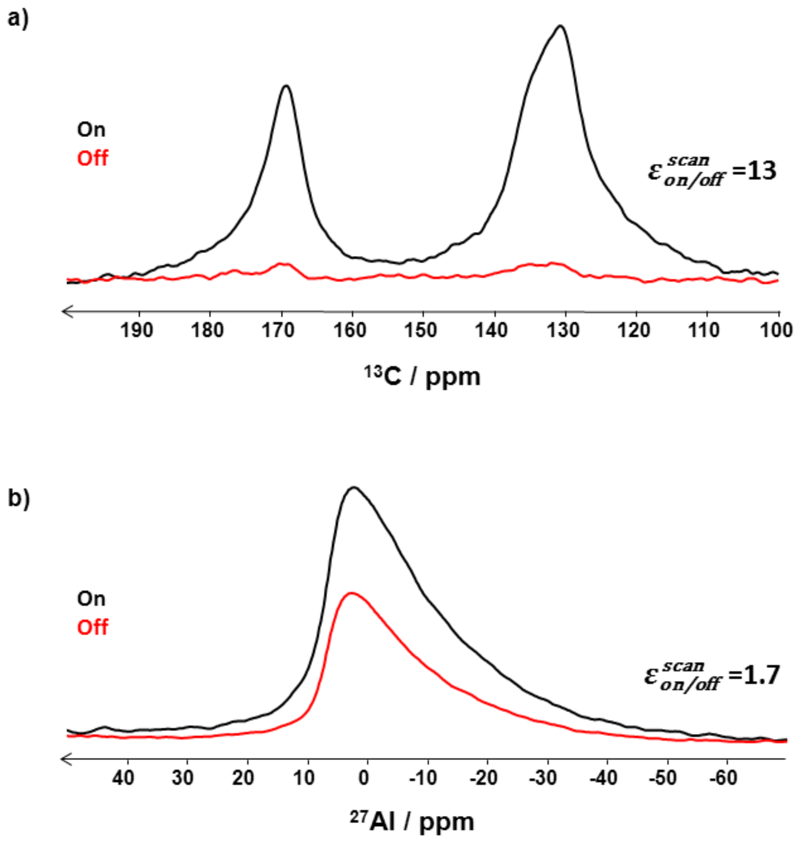

Fig.S4 (a) Direct polarization ^{13}C MAS spectra and (b) ^{27}Al Hahn echo spectra of MIL-100(Al) recorded with (black) and without (red) μw irradiation. The direct ^{13}C MAS spectra were acquired with a ^{13}C 90° pulse length of 6 μs and resulted from the accumulation of 128 transients with a recovery delay of 60 s, leading to a total experimental time of 128 min. The rf amplitude of ^{27}Al 90° and 180° CT-selective pulses was 5.5 kHz and the delay between the centers of these pulses was $\tau_r = 1/\nu_r$. The ^{27}Al Hahn echo NMR spectra resulted from the accumulation of 16 transients with a recovery delay of 1.5 s, leading to a total experimental time of 24 s.

DNP enhancement for direct ^{13}C MAS if TOTAPOL is outside MIL-100(Al) cavities

In MIL-100(Al) with natural isotopic abundance, the ^{13}C spin diffusion is vanishing and the DNP transfer is only conveyed by electron-^{13}C interaction. Therefore, the DNP transfer in direct ^{13}C MAS experiments is limited to a few nanometers.[12] Here, we consider a transfer depth of 5 nm. Assuming TOTAPOL is prevented from entering the cavities of MIL-100(Al), DNP in direct MAS experiment can only polarize the "outer" nuclei, located at a distance less than 5 nm from outer surface of MIL-100(Al) crystals. The molar fraction of "outer" ^{13}C nuclei can be estimated as[7]

$$x_{out} = 4\pi R^2 5 / \left[\frac{4}{3}\pi R^3\right] = \frac{15}{R} \tag{S11}$$

and the expected enhancement per scan due to μw irradiation is

$$\varepsilon_{on/off}^{scan} = 1 + x_{out}\left\lfloor \varepsilon_{on/off}^{scan}(R) - 1 \right\rfloor. \tag{S12}$$

With R = 500 nm and $\varepsilon_{on/off}^{scan} = 8.5$, Eqs.S11 and S12 yield $\varepsilon_{on/off}^{scan}(R) \approx 400$, which is significantly higher than DNP enhancements per scan reported for direct ^{13}C MAS at 9.4 T.[13] This inconsistency confirms again the presence of TOTAPOL within the cavities of MIL-100(Al).

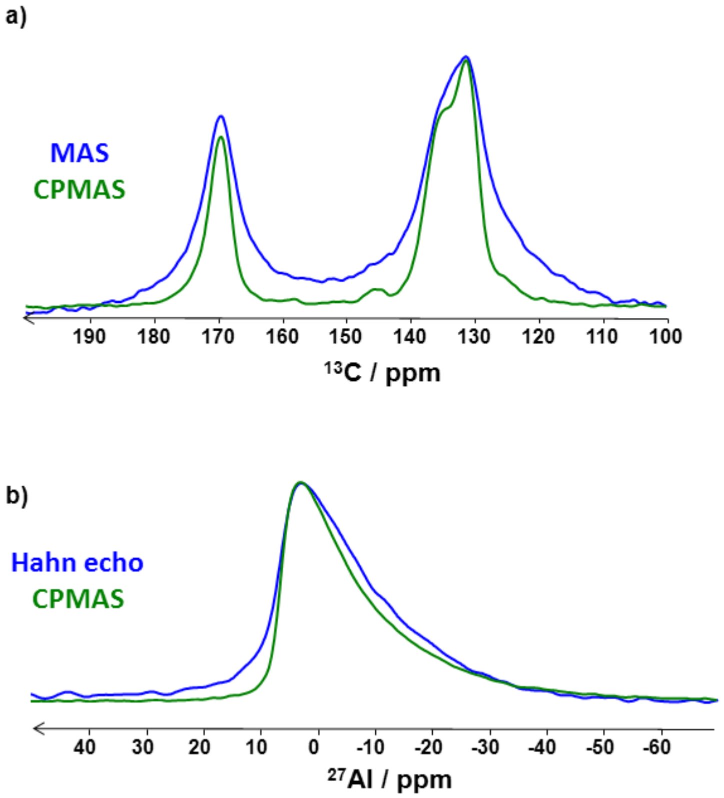

Fig.S5 (a) Comparison between direct ^{13}C MAS and ^{1}H→^{13}C CP-MAS spectra of MIL-100(Al) recorded with μw irradiation. (b) Comparison between ^{27}Al Hahn echo and ^{1}H→^{27}Al CP-MAS spectra of MIL-100(Al) recorded with μw irradiation. The CP-MAS spectra are identical to those of Fig.1 in the main text, whereas the direct ^{13}C MAS and ^{27}Al Hahn echo spectra are those of Fig.S4. Here, these spectra are scaled to the same absolute intensity to highlight changes in spectral resolution.

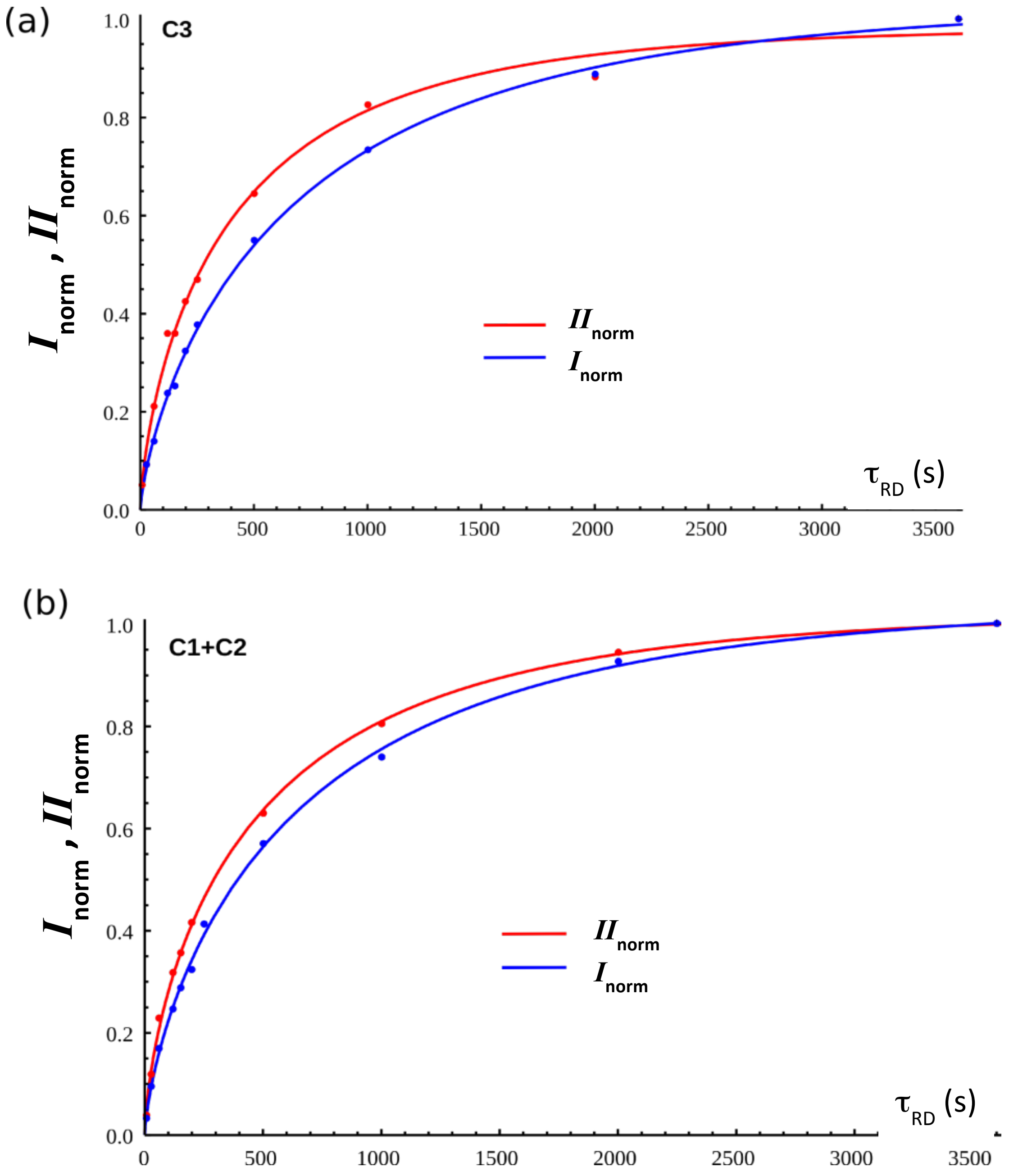

Fig.S6 Build-ups of intensity and intregrated intensity of DNP-enhanced direct ^{13}C MAS signals of (a) C3 and (b) C1,2 sites. The signal intensity, $I(\tau_{\mathrm{RD}})$, and the integrated intensity, $II(\tau_{\mathrm{RD}})$, are normalized with respect to their value at τ_{RD} = 3600 s: $X_{\mathrm{norm}}(\tau_{\mathrm{RD}}) = X(\tau_{\mathrm{RD}})/X(3600\mathrm{s})$ with $X = I$ and II. The experimental values are depicted as dots, whereas the best fit curves are displayed as continuous lines.

The buildups of I_{norm} and II_{norm} were fitted to a stretched exponential function

$$X_{\mathrm{norm}}(\tau_{\mathrm{RD}}) = X_{\mathrm{norm}}^{\infty}\left\{1-\exp\left[-\left(\frac{\tau_{\mathrm{RD}}}{T_1}\right)^{n}\right]\right\} \qquad \text{(S13)}$$

Where $X = I$ or II, $X_{\mathrm{norm}}^{\infty}$ is the asymptotic value of X, n is an integer number lower than 1, is T_1 is the build-up time constant. The best fit parameters T_1 and n for the C3 and C1,2 signals are given in Table S1.

Table S1. Parameters T_1 and n for the best fits of the buildup curves of DNP-enhanced direct MAS signals of C3 and C1,2 sites.

Sites	C3		C1,2	
X	*I*	*II*	*I*	*II*
n	0.75	0.71	0.73	0.72
T_1 /s	746	449	701	747

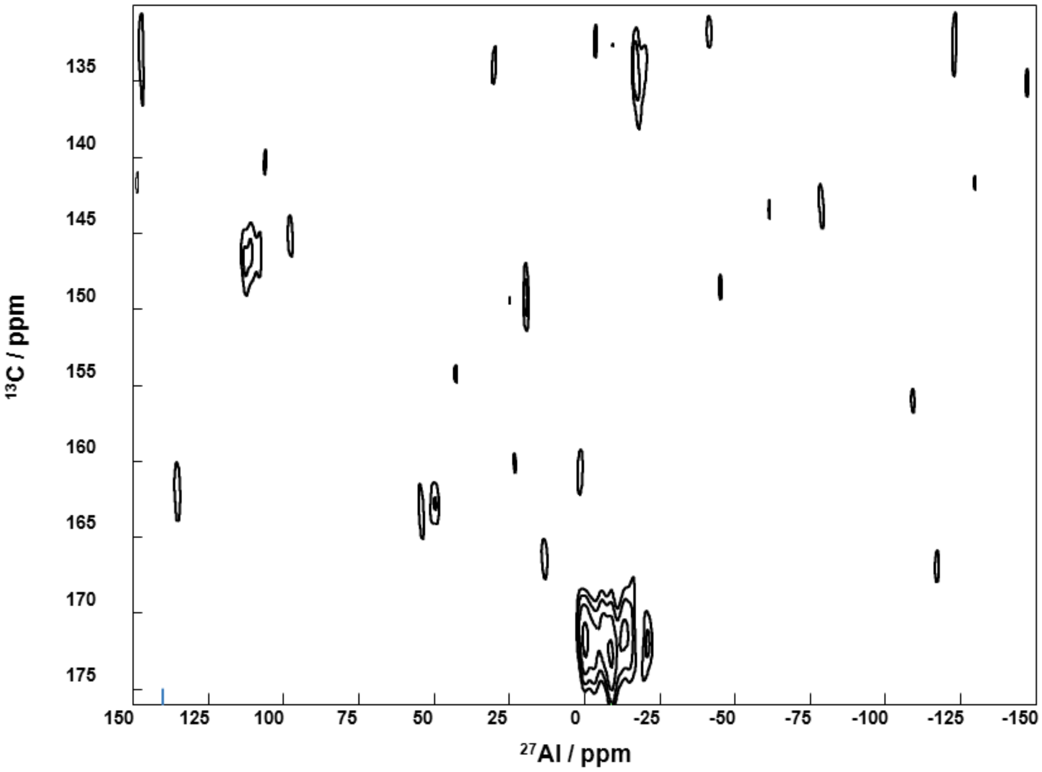

Fig.S7 ^{27}Al-{^{13}C} CP-*D*-HMQC spectrum recorded at 9.4 T, ν_r = 10 kHz and room temperature without μw irradiation.

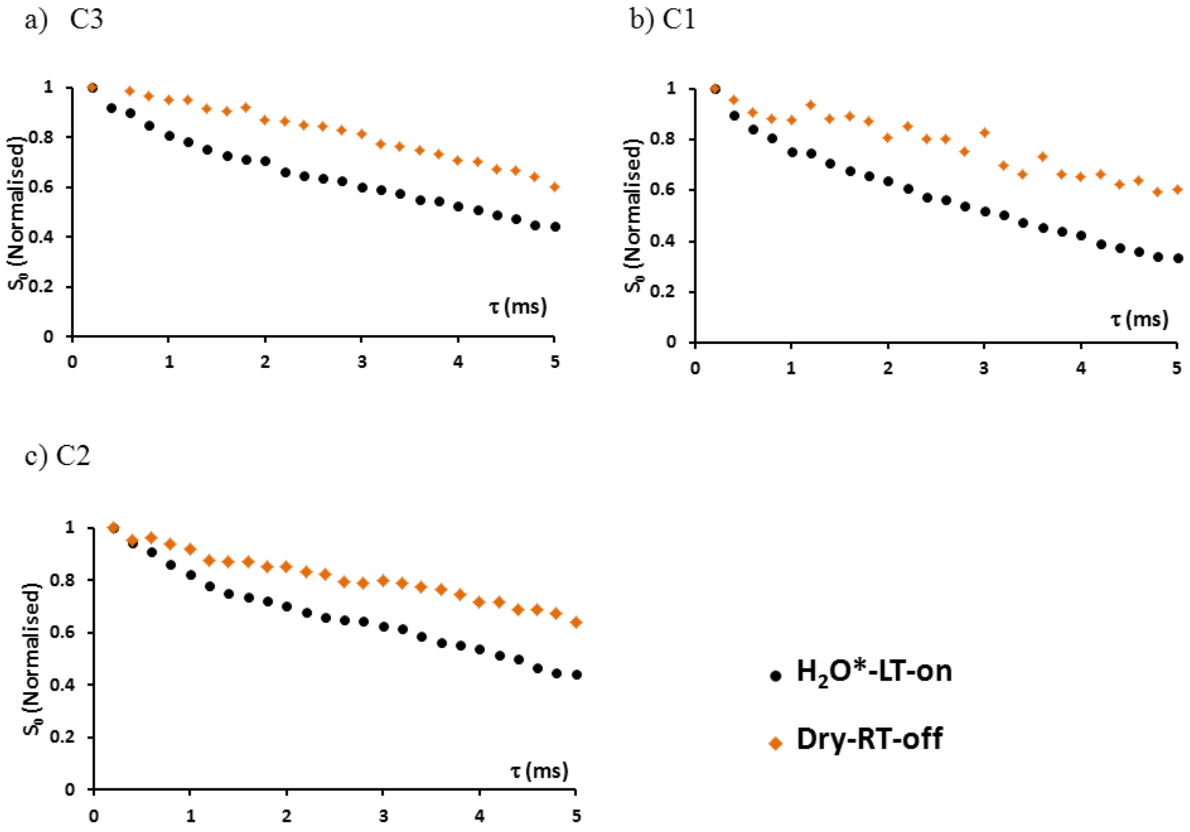

Fig.S8 Evolution of reference signals, S_0, for sites C1, C2 and C3 versus recoupling time, τ, of ^{27}Al-^{13}C S-RESPDOR experiments for experimental conditions H_2O*-LT-on (black disks) and dry-RT-off (orange diamond). For each site and condition, S_0 signal is normalized with respect to its value for τ = 0.

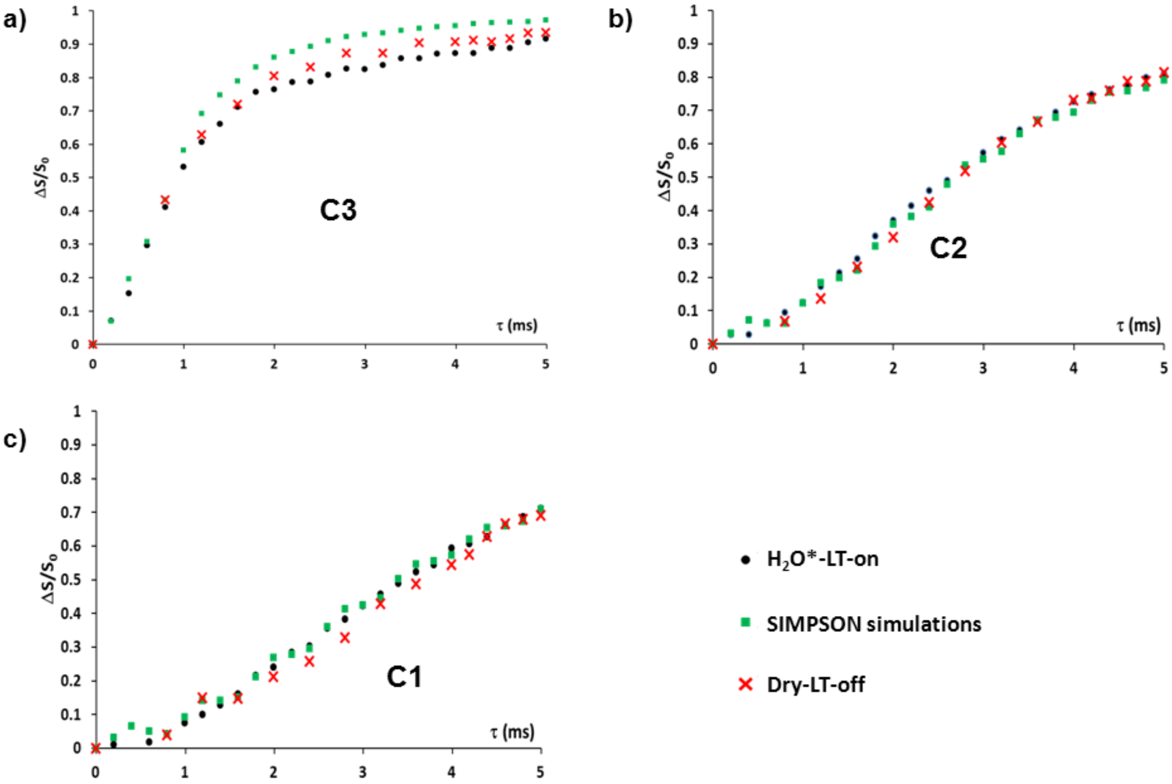

Fig.S9 Experimental ^{27}Al-^{13}C S-RESPDOR fraction curves of the three ^{13}C signals of H_2O*-LT-on (black disks) and dry MIL-100(Al) without microwave irradiation at 100 K (dry-LT-off, red crosses). ^{27}Al-^{13}C S-RESPDOR fraction curves simulated from the crystal structure of MIL-100(Al)[14] are also shown (green squares). Details about the simulation of ^{27}Al-^{13}C S-RESPDOR fraction curves are given above. There is an excellent agreement between experimental and simulated S-RESPDOR fraction curves for C1 and C2. The larger discrepancy for C3 stems from the presence of third Al neighbors, which were not included in the spin system for simulations.

Table S2. Average distances between each C*i* environment and its first and second nearest Al neighbours determined from the single crystal structure analysis of MIL-100(Al).

Site (δ_{iso} /ppm)	C3 (169)	C2 (131)	C1 (138)
d_1(C*i*-Al)[a] /nm	0.284	0.417	0.452
d_2(C*i*-Al)[b] /nm	0.290	0.420	0.458

[a] Average distance between C*i* environment with *i* = 1, 2 and 3 and the first nearest Al neighbour. [b] Average distance between C*i* environment and the second nearest Al neighbour.

1 C. Volkringer, D. Popov, T. Loiseau, G. Férey, M. Burghammer, C. Riekel, M. Haouas and F. Taulelle, *Chem. Mater.*, 2009, **21**, 5695.

2 Y. Matsuki, T. Maly, O. Ouari, H. Karoui, F. Le Moigne, E. Rizzato, S. Lyubenova, J. Herzfeld, T. Prisner, P. Tordo and R. G. Griffin, *Angew. Chem.-Int. Ed.*, 2009, **48**, 4996.

3 B. M. Fung, A. K. Khitrin and K. Ermolaev, *J. Magn. Reson.*, 2000, **142**, 97.

4 O. Lafon, Q. Wang, B. W. Hu, F. Vasconcelos, J. Trébosc, S. Cristol, F. Deng and J. P. Amoureux, *J. Phys. Chem. A*, 2009, **113**, 12864; X. Lu, O. Lafon, J. Trébosc, G. Tricot, L. Delevoye, F. Mear, L. Montagne and J. P. Amoureux, *J. Chem. Phys.*, 2012, **137**.

5 M. Bak, J. T. Rasmussen and N. C. Nielsen, *J. Magn. Reson.*, 2000, **147**, 296.

6 L. Chen, X. Y. Lu, Q. A. Wang, O. Lafon, J. Trébosc, F. Deng and J. P. Amoureux, *J. Magn. Reson.*, 2010, **206**, 269.

7 O. Lafon, A. S. L. Thankamony, T. Kobayashi, D. Carnevale, V. Vitzthum, I.I. Slowing, K. Kandel, H. Vezin, J. P. Amoureux, G. Bodenhausen and M. Pruski, *J. Phys. Chem. C*, 2013, **117**, 1375.

8 C. Volkringer, D. Popov, T. Loiseau, G. Férey, M. Burghammer, C. Riekel, M. Haouas and F. Taulelle, *Chem. Mater.*, 2009, **21**, 5695.

9 S. R. Rabbani and D. T. Edmonds, *Phys. Rev. B*, 1994, **50**, 6184; A. J. Rossini, A. Zagdoun, M. Lelli, J. Canivet, S. Aguado, O. Ouari, P. Tordo, M. Rosay, W. E. Maas, C. Coperet, D. Farrusseng, L. Emsley and A. Lesage, *Angew. Chem-Int. Ed.*, 2012, **51**, 123.

10 O. Lafon, M. Rosay, F. Aussenac, X. Y. Lu, J. Trébosc, O. Cristini, C. Kinowski, N. Touati, H. Vezin and J. P. Amoureux, *Ang. Chem-Int. Ed*, 2011, **50**, 8367; D. Lee, H. Takahashi, A. S. L. Thankamony, J. P. Dacquin, M. Bardet, O. Lafon and G. De Paepe, *J. Am. Chem. Soc.*, 2012, **134**, 18491.

11 T. Kobayashi, O. Lafon, A. S. L. Thankamony, I.I. Slowing, K. Kandel, D. Carnevale, V. Vitzthum, H. Vezin, J. P. Amoureux, G. Bodenhausen and M. Pruski, *Phys. Chem. Chem. Phys.*, 2013, **15**, 5553.

12 O. Lafon, A. S. L. Thankamony, M. Rosay, F. Aussenac, X. Y. Lu, J. Trébosc, V. Bout-Roumazeilles, H. Vezin and J. P. Amoureux, *Chem. Commun.*, 2013, **49**, 2864.

13 U. Akbey, W. T. Franks, A. Linden, S. Lange, R. G. Griffin, B. J. van Rossum and H. Oschkinat, *Angew. Chem.-Int. Ed.*, 2010, **49**, 7803.

14 C. Volkringer, T. Loiseau, M. Haouas, F. Taulelle, D. Popov, M. Burghammer, C. Riekel, C. Zlotea, F. Cuevas, M. Latroche, D. Phanon, C. Knofelv, P. L. Llewellyn and G. Férey, *Chem. Mater.*, 2009, **21**, 5783.